Elsevier Editorial System(tm) for Chemical Physics Letters

Manuscript Draft

Manuscript Number:

Title: Fluorescence study of the effect of the oxidized phospholipids on amyloid fibril formation by the apolipoprotein A-I N-terminal fragment

Article Type: Research paper

Section/Category: Biomolecules

Corresponding Author: Mrs. Kateryna Vus, Ph.D.

Corresponding Author's Institution: V.N. Karazin Kharkiv National University

First Author: Kateryna Vus, Ph.D.

Order of Authors: Kateryna Vus, Ph.D.; Mykhailo Girych; Valeriya Trusova; Galyna Gorbenko; Paavo Kinnunen; Chiharu Mizuguchi; Hiroyuki Saito

Abstract: The effects of the oxidized phospholipids (oxPLs) on amyloid fibril formation by the apolipoprotein A-I variant 1-83/G26R have been investigated using Thioflavin T fluorescence assay. All types of the PoxnoPC assemblies (premicellar aggregates, micelles, lipid bilayer vesicles) induced the enhancement the 1-83/G26R fibrillization, although PazePC micelles completely prevented protein aggregation at low protein-to-lipid molar ratios. Furthermore, 1-83/G26R fibrillization in the presence of the oxPLs was accompanied by the retardation of amyloid nucleation and elongation. Notably, the ability of PazePC to inhibit the formation of 1-83/G26R fibrils was explained by the protein-lipid-electrostatic interactions, stabilizing the α-helical structure of membrane/micelle-associated 1-83/G26R.

Suggested Reviewers: Eva Žerovnik PhD
Assistant professor, Department of Biochemistry, Molecular and Structural Biology, J. Stefan Institute, Jamova 39, SI-1000 Ljubljana, Slovenia
eva.zerovnik@ijs.si
Expert in amyloid research.

Olga Gursky PhD
Professor, Department of Physiology and Biophysics, Boston University School of Medicine
gursky@bu.edu
Expert in human high-, low- and very-low-density lipoprotein biophysics.

Jelena Kirilova PhD
Associate Professor , Faculty of Natural Sciences and Mathematics, Daugavpils University
elena.kirilova@inbox.lv
Expert in fluorescence spectroscopy.

The present paper provides an insight into the amyloid fibril formation by the apolipoprotein A-I N-terminal fragment in the presence of the oxidized phospholipids (oxPLs). Using Thioflavin T assay, the kinetic parameters of the protein fibrillization have been revealed. The novelty of the results obtained is as follows: i) the effects of the oxPLs varied with the lipid structure, concentration and the type of lipid assemblies; ii) PazePC micelles completely inhibited protein fibrillization; iii) a model for the association between the 1-83/G26R and POPC/PazePC bilayer has been suggested.

***Highlights (for review)**

- Oxidative stress plays a critical role in Alzheimer's, Parkinson's diseases, etc.
- Apolipoprotein A-I (ApoA-I) G26R mutation is associated with hereditary amyloidosis.
- Oxidized phospholipids modulated amyloid fibril formation by ApoA-I 1-83/G26R.
- PazePC micelles stabilized α-helical structure of ApoA-I 1-83/G26R.

*Graphical Abstract (pictogram) (for review)

Click here to download high resolution image

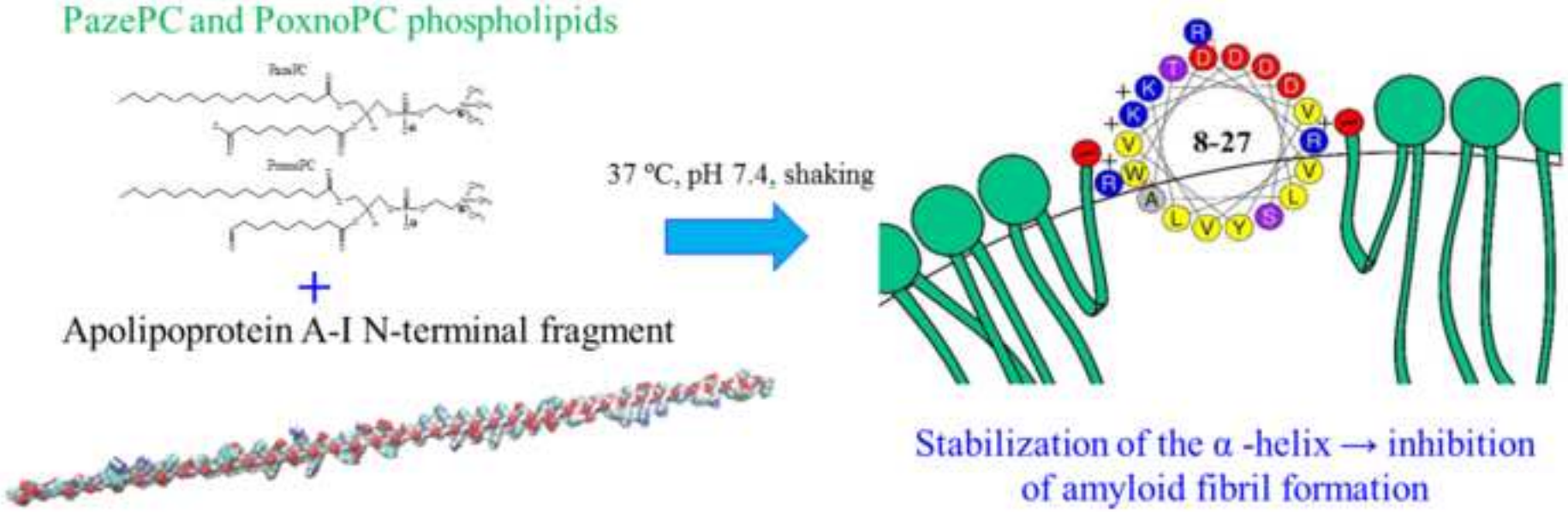

Fluorescence study of the effect of the oxidized phospholipids on amyloid fibril formation by the apolipoprotein A-I N-terminal fragment

Kateryna Vus[1*], Mykhailo Girych[2], Valeriya Trusova[1], Galyna Gorbenko[1], Paavo Kinnunen[3], Chiharu Mizuguchi[4], Hiroyuki Saito[4]

[1]Department of Nuclear and Medical Physics, V.N. Karazin Kharkiv National University, 4 Svobody Sq., Kharkiv 61022, Ukraine; [2]Department of Physics, University of Helsinki, 2a Gustaf Hällströmin katu, Helsinki, FIN-00014, Finland; [3]Department of Neuroscience and Biomedical engineering, School of Science and Technology, Aalto University, 3J Otakaari, Espoo, FI-00076, Finland; [4]Nakauchi-cho, Misasagi, Yamashina-ku, Kyoto 607-8414, Japan, 5 Department of Biophysical Chemistry, Kyoto Pharmaceutical University

Abstract

The effects of the oxidized phospholipids (oxPLs) on amyloid fibril formation by the apolipoprotein A-I variant 1-83/G26R have been investigated using Thioflavin T fluorescence assay. All types of the PoxnoPC assemblies (premicellar aggregates, micelles, lipid bilayer vesicles) induced the enhancement the 1-83/G26R fibrillization, although PazePC micelles completely prevented protein aggregation at low protein-to-lipid molar ratios. Furthermore, 1-83/G26R fibrillization in the presence of the oxPLs was accompanied by the retardation of amyloid nucleation and elongation. Notably, the ability of PazePC to inhibit the formation of 1-83/G26R fibrils was explained by the protein-lipid- electrostatic interactions, stabilizing the α-helical structure of membrane/micelle-associated 1-83/G26R.

[*]Address for correspondence:
38-12 Aeroflotskaya Str., Kharkiv,
61031, Ukraine
E-mail: kateryna_vus@yahoo.com
Tel: (+380 57) 3438244

1. Introduction

The oxidative stress is known to play a critical role in a wide variety of pathological states including the amyloid disorders, such as Alzheimer's (AD), Parkinson's (PD), Creutzfeldt–Jakob diseases (CJD), systemic amyloidosis (SA), etc. Furthermore, the damage of proteins, lipids and DNA by reactive oxygen species (ROS) precede the appearance of a major hallmark of these pathologies, amyloid fibril formation by specific proteins, Aβ peptide (AD), α-synuclein (PD), prion protein (CJD), lysozyme (SA), etc. [1-4]. To exemplify, Aβ peptide interactions with transition metal ions (viz. iron, copper, zinc, whose levels are elevated in AD brain), has been shown to result in ROS production followed by the enhanced Aβ aggregation [1,5]. The increased oxidative environment of dopaminergic neurons has been reported to induce α-synuclein fibrillization and mitochondria damage in neurons, the processes being involved in the etiology of PD [6]. The lysozyme oxidation promoted the amyloid fibril formation *in vitro*, etc. [4,7].

Apolipoprotein A-I (apoA-I) is the main component of the plasma high density lipoproteins (HDL) involved in the two main processes: i) transferring the excess of cholesterol to the liver (reverse cholesterol transport) [8]; and ii) mediating the antioxidative processes in the low density lipoproteins (LDL) [9,10]. The HDL oxidation by myeloperoxidase in patients with established atherosclerosis has been demonstrated to limit their ability to participate in the reverse cholesterol transport [11]. Furthermore, the oxidation of methionine residues of apoA-I and genetic mutations, particularly, Iowa mutation (G26R) resulted in the amyloid fibril formation, associated with low HDL level and hereditary amyloidosis [12,13].

Protein amyloidogenesis has been proved to be a membrane-associated process, with lipid bilayer acting as a matrix which favours the aggregation-competent conformation of the polypeptide chain, interfacial accumulation and specific orientation of membrane-bound proteins [14,15]. Of great interest in this context is the modulation of amyloid fibril formation by the oxidatively damaged membranes, possessing the extended lipid conformation, altered polarity profile, lowered energy barrier for lipid flip-flop, etc. [16,17]. For instance, the fibrillization of Aβ peptide and gelsolin, was enhanced in the presence of the oxPLs presumably due to the Schiff-base or β-sheet formation, respectively, followed by the protein aggregation [18,19]. The above studies reported protein fibrillization in the presence of two stable lipid oxidation products, namely 1-palmitoyl-2-azelaoyl-sn-glycero-3-phosphocholine (PazePC) and 1-palmitoyl-2-(9'-oxononanoyl)-sn-glycero-3-phosphocholine (PoxnoPC). According to the molecular dynamic simulations, in the lipid bilayer the polar chain of PazePC is oriented in such a manner that the carboxyl group is located in the aqueous phase, while the carbonyl group of PoxnoPC resides in the glycerol backbone region [20]. The fact that the reactive groups of these

compounds are localized near the membrane surface could explain the observed pronounced effects of the oxPLs on the amyloid fibril formation. However, the precise mechanisms underlying the such effects remain largely unknown. Some metal oxides have been reported to inhibit amyloid fibril formation, suggesting the complex nature of oxidative modification of the protein structure [21]. Our recent studies showed that the lipid bilayers containing PoxnoPC, trigger insulin fibrillization at physiological pH, while those containing PazePC, inhibit this process as compared to the POPC bilayers [22]. Interestingly, the oxPLs dispersions induced a more pronounced enhancement of the lysozyme amyloid formation than liposomes, being accompanied by the increase of the lag time [22]. The finding that the the oxidized phospholipids can not only promote, but also suppress amyloid nucleation and growth, render them potential candidates for anti-amyloid agents. To gain deeper insight into the effects of PazePC and PoxnoPC on the amyloid formation, we further extended our investigations to the N-terminal 1-83 fragment of human apolipoprotein A-I (1-83) and its aggregation-competent variant G26R (1-83/G26R) [12]. More specifically, the present study was aimed at monitoring the kinetics of 1-83/G26R fibrillization *in vitro* using Thioflavin T assay and testing the ability of the oxPLs to inhibit the amyloid growth. Our goals were: i) to estimate the kinetic parameters of the protein aggregation in the presence of lipids; ii) to compare the effects of the oxPLs-containing liposomes, micelles and dispersions on 1-83 and 1-83/G26R fibrillization; iii) to uncover the role of the G26R mutation in the oxPLs-mediated amyloidogenesis of the N-terminal 1-83 fragment of apolipoprotein A-I.

2. Materials and methods

Materials

The N-terminal 1-83 fragment of human apolipoprotein A-I (1-83) and its variant G26R (1-83/G26R) were expressed and purified as described previously [12,23]. Thioflavin T was from Molecular Probes (Oregon, USA). The dye stock solution was prepared in Tris-HCl buffer (150 mM NaCl, 0.01 % NaN_3, pH 7.4). ThT concentration was determined spectrophotometrically using the extinction coefficient $\varepsilon_{412} = 23800\ M^{-1}cm^{-1}$. 1-palmitoyl-2-azelaoyl-sn-glycero-3-phosphocholine (PazePC), 1-palmitoyl-2-(9'-oxononanoyl)-sn-glycero-3-phosphocholine (PoxnoPC), and 1-palmitoyl-2-oleoyl-sn-glycero-3-phosphocholine (POPC) lipids were from Avanti Polar Lipids (Alabaster, AL). The structures of the used lipids are shown in Fig. 1.

Preparation of lipid dispersions, micelles and vesicles

Lipid dispersions and vesicles were obtained as described previously [24]. Briefly, the sonication was employed to obtain lipid dispersions (below and above critical micelle

concentration). The 100-nm lipid vesicles from POPC and its mixtures with PazePC (20 mol%) or PoxnoPC (20 mol%) were prepared by the extrusion technique.

The kinetics of amyloid formation monitored by Thioflavin T assay

The apoA-I N-terminal fragments 1-83 and 1-83/G26R were freshly dialyzed from 6 M guanidine hydrochloride solution into 10 mM Tris buffer (150 mM NaCl, 0.01 % NaN_3, pH 7.4) before use. The kinetics of amyloid formation by the 1-83 and 1-83/G26R fragments was monitored by Thioflavin T assay. Specifically, 96-well plates (Frickenhausen, Germany) filled with the dye (10 μM), proteins (5 μM) and lipids (0 – control samples, 0.5, 5 or 50 μM) were loaded into a fluorescence microplate reader (SPECTRAFluor Plus, Tecan, Austria), heated to 37 ºC and incubated under constant shaking up to several days. ThT fluorescence was recorded over time at 485 nm (10 nm bandpass filter) using excitation at 430 nm (35 nm bandpass filter).

The quantitative characteristics of the fibrillization process were obtained by approximating the time (t) dependence of ThT fluorescence intensity at 485 nm (F) with the sigmoidal curve [12]:

$$F = F_0 + \frac{F_{\max} - F_0}{1 + \exp[k(t_m - t)]}, \quad (1)$$

where F_0 and $F_{\max}$ are ThT fluorescence intensities in the free form and in the presence of protein after the saturation has been reached, respectively; k is the apparent rate constant for the fibril growth; t_m is the time needed to reach 50% of maximal fluorescence. The lag time was calculated as: $t_m - 2/k$.

3. Results and discussion

As seen in Fig. 2, the effect of the oxidized phospholipids on the fibrillization of 1-83/G26R varies with the lipid structure and concentration. Specifically, the most pronounced (up to ~3 times) increase in the maximum Thioflavin T fluorescence $F_{\max}$, which is proportional to the extent of fibril formation, was observed at the protein-to-lipid molar ratio 1:1 (Table 1) [25]. Likewise, above the critical micelle concentration (at lipid concentration 50 μM), the lowest $F_{\max}$ values were recovered [26]. The fact that below the CMC Thioflavin T fluorescence was proportional to the lipid concentration, while above the CMC it substantially decreased, agree with the results reported by Mahalka et al. for the fibrillization of gelsolin fragments, induced by PoxnoPC [27]. Furthermore, this tendency was also observed for the insulin fibrillization in the presence of PazePC [22]. Notably, the opposite effects of the PoxnoPC and PazePC on the 1-83/G26R aggregation at the lipid concentrations 5 μM and 50 μM could be attributed to the different mechanisms of the protein interaction with premicellar aggregates and micelles [27].

Next, both oxPLs slowed down the 1-83/G26R nucleation, resulting in a substantial increase in the lag time (up to 3-fold) and decrease in the fibrillization rate k (up to 5-fold), as compared to the control samples (Table 1). Similarly, the extension of the lag time was observed for $FtG_{179–194}$ gelsolin fragment in the presence of PoxnoPC [27]. These results suggest the ability of the examined oxPLs to form stable complexes with apoA-I N-terminal fragment, hampering the formation of amyloid nuclei and stabilizing the protein oligomers [28].

Furthermore, at the protein-to-lipid molar ratio 1:1, PazePC induced less pronounced enhancement of the 1-83/G26R fibrillization than PoxnoPC. The former also exerted inhibiting effect on the protein fibrillization at the smaller or greater protein-to-lipid molar ratios (Table 1). Specifically, no change in ThT fluorescence was observed upon the 1-83/G26R incubation in the presence of 50 μM PazePC, indicating that lipid micelles prevent the protein fibrillization. Similarly, Mahalka et al. demonstrated that PazePC did not have a noticeable influence on the fibrillization of $FtG_{179–194}$ gelsolin fragment, while PoxnoPC promoted the peptide aggregation [27]. In turn, PazePC enhanced the amyloid formation by the lysozyme and insulin, showing a more significant effect on the insulin aggregation than PoxnoPC [22]. This may result from the specific interactions of the carboxyl group of PazePC with insulin, inducing its partial denaturation and transition into the aggregation-prone conformation [22]. As the G26R mutation promotes amyloid fibril formation through the destabilization of the α-helical structure of the 1-83/G26R fragment associated with lipid bilayer, the 1-83/G26R binding to PazePC micelles could induce the opposite effect, preventing the protein aggregation [11].

As seen in Fig. 3, the lag time of amyloid fibril formation by 1-83/G26R in the absence of lipids was about 3 times smaller, and the fibrillization rate was 6 times greater, as compared to the correspondent values for the 1-83 aggregation. These results are in harmony with the data of Adachi et al., suggesting that G26R mutation enhanced the amyloid fibril formation [11]. Furthermore, the apparent rate constant for the 1-83 fibril growth in the presence of the oxPLs was twice than its control value, the lag time was increased 2-fold, and the fibrillization extent was reduced (Table 1). Thus, similarly to the 1-83/G26R, the 1-83 forms a smaller number of fibrils in the presence of PazePC micelles.

In the following, the effect of lipid vesicles composed of POPC and its mixtures with the oxPLs on the 1-83/G26R amyloid fibril formation has been evaluated. As seen in Fig. 4 and Table 1, the addition of liposomes to the protein solution induced ~2-fold increase of the F_{max}, ~3–5-fold decrease of the k value, and ~9–12-fold extension of the lag time. This tendency is in good agreement with the previously reported data obtained for $FtG_{179–194}$ gelsolin fragment and insulin [22,27]. Specifically, PoxnoPC and PazePC incorporated into the liposomal membranes

slowed down the kinetics of amyloid fibril formation, as compared to the control samples and lipid dispersions [22,27].

Furthermore, the effects of POPC, POPC/PazePC(20 mol%) and POPC/PoxnoPC(20 mol%) on the 1-83/G26R aggregation did not vary significantly, although inclusion of PazePC into POPC bilayer resulted in the ~40% decrease in the fibrillization extent, as compared to the neat POPC liposomes (Table 1). Notably, the fact that PazePC micelles prevented amyloid fibril formation by the apoA-I amyloidogenic fragment at the low lipid-to-protein weight ratio ~ 0.8 (Fig. 2), while POPC/PazePC (20 mol%) liposomes slowed down the kinetics of the protein aggregation (Fig. 4), suggest that the observed effects are governed by specific PazePC-1-83/G26R interactions with the lipid bilayers or micelles. These results, together with those reported for $FtG_{179–194}$ gelsolin fragment, highlight a critical role of PazePC in inhibiting the amyloid fibril formation by the short (unstructured) peptides [27], although this lipid seems to induce misfolding and aggregation of the full-length proteins, like lysozyme or insulin, more effectively than PoxnoPC [22]. Interestingly, the oxPLs have been found to accelerate the amyloid nucleation, presumably due to the perturbation of the membrane structure and dynamics by the oxidized lipid tails [29].

Recently, Saito et al. have reported the enhancement of the 1-83/G26R aggregation on POPC membranes produced by the G26R amyloidogenic mutation [25]. In contrast, no ThT fluorescence response was observed in the case of 1-83 at the lipid-to-protein weight ratio ~ 30. Our study indicates that the 1-83/G26R still retains the ability to form amyloid fibrils in the presence of vesicles containing the oxPLs at the lipid-to-protein weight ratio ~ 31 (Fig. 4). It can be assumed that there exist the α-helixes formed by the unstructured 1-83/G26R on the membrane surface, which are destabilized regardless of the presence of PazePC [11,25]. Such a destabilization induced by the G26R mutation promotes further transformation of the helixes into the β-sheets, followed by the amyloid fibril formation on the membrane surface, being a common mechanism for the natively unstructured proteins and peptides involved in amyloid pathologies [30–32].

Finally, in order to explain the decrease of the 1-83/G26R fibrillization extent induced by the POPC/PazePC (20 mol%) vesicles (micelles), a model for the association between the 1-83/G26R and POPC/PazePC bilayer has been suggested (Fig. 5). According to this model, the nonpolar faces of the amphipathic helixes of the ApoA-I N-terminal fragment, interact with the lipid bilayer while their polar faces are in contact with the aqueous phase [33,34]. The two panels in Fig. 5 are the helical wheel projections of the residues 8–27 and 36–65, containing the most aggregation-prone regions 14–22 and 49–57 [25]. Obviously, the positively charged amino acid residues of the ApoA-I N-terminal fragment could associate with the sn-2 chain of PazePC

extended into the aqueous phase via strong electrostatic interactions [20,29]. This may increase free energy of denaturation of the α-helixes and, as a consequence, reduce the fibrillization extent, as compared to the neat POPC vesicles. Notably, it is PazePC interaction with the residue R26 that could be critical for the inhibition of the 1-83/G26R aggregation by the oxidized phospholipids [25]. Unlike lipid vesicles, micelles are composed only of the PazePC molecules, resulting in the increased number of the protein-lipid electrostatic contacts on the micelle surface and the complete inhibition of the 1-83/G26R aggregation. Interestingly, PoxnoPC micelles induced a less pronounced increase in the 1-83/G26R fibrillization, compared to the lipid dispersions (Fig. 2B), being indicative of their potential to inhibit amyloid fibril formation by specific interactions with the protein at higher lipid-to-protein molar ratios, than PazePC. Furthermore, since the 1-83/G26R is unstructured in solution, its electrostatic interactions and Schiff base formation with PazePC and PoxnoPC dispersions, respectively, could result in the protein cross-linking, nucleation and lipid embedding into the oligomers and amyloid fibrils [27,35]. The above processes may lead to the experimentally observed enhancement of the 1-83/G26R fibrillization with the concentration of lipid dispersions (Table 1). In turn, significant increase in the lag time of the 1-83/G26R amyloid formation in the presence of lipid vesicles used in this study seems to result from the lowered protein concentration on the membrane surface, but not due to the stabilization of the protein α-helical conformation, as was suggested for the lipid dispersions and micelles [25].

4. Conclusions

In conclusion, our fluorescence studies demonstrated that the kinetic parameters of the 1-83/G26R fibrillization varied significantly with the oxPLs structure, concentration and the type of lipid assemblies (premicellar aggregates, micelles or lipid bilayer vesicles). Specifically, membrane/micelle surfaces were found to play a critical role in inhibition of the amyloid fibril formation, presumably due to their ability to stabilize α-helical structure of the 1-83/G26R by the protein-lipid electrostatic and covalent interactions. Furthermore, the increase in the lag time of the 1-83/G26R fibrillization induced by the oxPLs suggest that their binding to the protein hampered the formation of amyloid nuclei. Overall, the results obtained indicate that despite the involvement of the oxidative stress into pathogenesis of amyloid diseases, the oxidized phospholipids can be regarded as candidates for novel anti-amyloid agents.

Acknowledgements

This work was supported by the Ministry of Education and Science of Ukraine (the Young Scientist project “Design of the novel methods of fluorescence diagnostics of amyloid pathologies”, project number: 0116U000937).

References

[1] P. Poprac, K. Jomova, M. Simunkova, V. Kollar, C.J. Rhodes, M. Valko, Trends Pharmacol. Sci. 38 (2017) 592.

[2] T. Jiang, Q. Sun, S. Chen, Prog. Neurobiol. 147 (2016) 1.

[3] S. Chen, S. He, J.K. Shang, M.M. Ma, C.S. Xu, X.H. Shi, J.W. Zhang, Clin. Biochem. 49 (2016) 292.

[4] S. Ghosh, N.K. Pandeya, S. Bhattacharya, A. Roy, N.V. Nagyc, S. Dasgupta, Int. J. Biol. Macromol. 76 (2015) 1.

[5] D.J. Bonda, H. Lee, J.A. Blair, X. Zhu, G. Perry, M.A. Smith, Metallomics. 3 (2011) 267.

[6] G.B. Irvine, O.M. El-Agnaf, G.M. Shankar, D.M. Walsh, Mol. Med. 14 (2008) 451.

[7] M.S. Petrônio, V.F. Ximenes. Biochim. Biophys. Acta. 1824 (2012) 1090.

[8] A.R. Tall, J. Intern. Med. 263 (2008) 256.

[9] A. Kontush, S. Chantepie, M.J. Chapman, Arteriosclerosis, Thrombosis, and Vascular Biology. 23 (2003) 1881.

[10] M. Navab, S.Y. Hama, C.J. Cooke, G.M. Anantharamaiah, M. Chaddha, L. Jin, G. Subbanagounder, K.F. Faull, S.T. Reddy, N.E. Miller, A.M. Fogelman, J. Lipid Res. 41 (2000) 1481.

[11] E. Adachi, H. Nakajima, C. Mizuguchi, P. Dhanasekaran, H. Kawashima, K. Nagao, K. Akaji, S. Lund-Katz, M.C. Phillips, H. Saito, J. Biol. Chem. 288 (2013) 2848.

[12] B. Shao, G. Cavigiolio, N. Brot, M.N. Oda, J.W. Heinecke, Proc. the National Academy of Sci. of the United States of America. 105 (2008) 12224.

[13] N.A. Ramella, G.R. Schinella, S.T. Ferreira, E.D. Prieto, M.E. Vela, J.L. Rios, M.A. Tricerri, O.J. Rimoldi, PLoS One 7 (2012) e43755.

[14] M. Stefani, Int. J. Mol. Sci. 9 (2008) 2515.

[15] C. Aisenbrey, T. Borowik, R. Byström, M. Bokvist, F. Lindström, H. Misiak, M.-A. Sani, G. Gröbner, Europ. Biophys. J. 37 (2008) 247.

[16] J.D. Knight, A.D. Miranker, J. Mol. Biol. 341 (2004) 1175.

[17] R. Volinsky, L. Cwiklik, P. Jurkiewicz, M. Hof, P. Jungwirth, P.K.J. Kinnunen, Biophys. J. 101 (2011) 1376.

[18] V. Koppaka, P.H. Axelsen, Biochemistry 39 (2000) 10011.

[19] P.K. Kinnunen, K. Kaarniranta, A.K. Mahalka, Biochim. Biophys. Acta 1818 (2012) 2446.

[20] H. Khandelia, O.G. Mouritsen, Biophys. J. 96 (2009) 2734.

[21] A. Bellova, E. Bystrenova, M. Koneracka, P. Kopcansky, F. Valle, N. Tomasovicova, M. Timko, J. Bagelova, F. Biscarini, Z. Gazova, Nanotechnology. 21 (2010) 065103.

[22] K.Vus, R. Sood, G. Gorbenko, P. Kinnunen, Methods Appl. Fluoresc. 4 (2016) 034008.

[23] M. Girych, G. Gorbenko, V. Trusova, E. Adachi, C. Mizuguchi, K. Nagao, H. Kawashima, K. Akaji, S. Lund-Katz, M.C. Phillips, H. Saito, J. Struct Biol. 185 (2014) 116.

[24] N.-J. Cho, L.Y. Hwang , J.J.R. Solandt, C.W. Frank, Materials 6 (2013) 3294.

[25] C. Mizuguchi, F. Ogata, S. Mikawa, K. Tsuji, T. Baba, A. Shigenaga, T. Shimanouchi, K. Okuhira, A. Otaka, H. Saito, J. Biol. Chem. 290 (2015) 20947.

[26] J.-P. Mattila, K. Sabatini, P.K.J. Kinnunen, Biophys. J. 93 (2007) 3105.

[27] A.K. Mahalka, C.P.J. Maury, P.K. J. Kinnune, Biochemistry. 50 (2011) 4877.

[28] A.S. Johansson, A. Garlind, F. Berglind-Dehlin, G. Karlsson, K. Edwards, P. Gellerfors, F. Ekholm-Pettersson, J. Palmblad, L. Lannfelt, FEBS J. 274 (2007) 990.

[29] R. Volinsky, P.K. Kinnunen, FEBS J. 280 (2013) 2806.

[30] G.P. Gorbenko, P.K. Kinnunen, Chem. Phys. Lipids. 141 (2006) 72.

[31] S.V. Verevka, Parametabolic β-aggregation of proteins: familiar mechanisms with diverse sequels, in Advances in Medicine and Biology, Nova Science Publishers, N.Y., 2013, Vol. 72, P. 29-48.

[32] E.R. Georgieva, T.F. Ramlall, P.P. Borbat, J.H. Freed, D. Eliezer, J. Biol. Chem. 285 (2010), 28261.

[33] W.S. Davidson, T.B. Thompson, J. Biol. Chem. 282 (2007), 22249.

[34] C. G. Brouillette, G.M. Anantharamaiah, J.A. Engler, D.W. Borhani, Biochim. Biophys. Acta. 1531 (2001), 4.

[35] L.M. Sayre, M.A. Smith, G. Perry, Curr. Med. Chem. 8 (2001), 721.

Legends to figures

Fig. 1. Structures of 1-palmitoyl-2-oleoyl-sn-glycero-3-phosphocholine (POPC), 1-palmitoyl-2-azelaoyl-sn-glycero-3-phosphocholine (PazePC) and 1-palmitoyl-2-(9'-oxononanoyl)-sn-glycero-3-phosphocholine (PoxnoPC).

Fig. 2. Fibrillization kinetics of the apoA-I 1-83/G26R variant in the absence or presence of PazePC (A – experimental, C – fitted curves) and PoxnoPC (B – experimental, D – fitted curves) lipid dispersions: 1 – no lipid, 2,3,4 – correspond to protein-to-lipid molar ratios 10:1, 1:1 and 1:10, respectively. Protein concentration was 5 μM, ThT concentration was 10 μM. PazePC and PoxnoPC concentrations were 0.5 μM, 5 μM and 50 μM.

Fig. 3. Fibrillization kinetics of the apoA-I 1-83 (A) and 1-83/G26R (B) variants in the absence or presence of PazePC and PoxnoPC lipid dispersions: 1 – no lipid, 2 – PazePC, 3 – PoxnoPC. Protein concentration was 5 μM, ThT concentration was 10 μM. PazePC and PoxnoPC concentrations were 50 μM, corresponding to the protein-to-lipid molar ratio 1:10.

Fig. 4. Fibrillization kinetics of the apoA-I 1-83/G26R variant in the presence of: 1 – POPC, 2 – POPC/PazePC (20 mol%), 3 – POPC/ PoxnoPC (20 mol%) liposomes (A – experimental, B – fitted curves). Protein concentration was 5 μM, ThT concentration was 10 μM. Liposome concentration was 2 mM, corresponding to POPC-to-apoA-I weight ratio ~ 31.

Fig. 5. Schematic illustration of the model for the association between 1-83/G26R and POPC/PazePC (20 mol%) bilayer. The black line represents the hydrophilic-hydrophobic interface of the bilayer leaflet.

Table 1

Kinetic parameters of amyloid formation by apoA-I 1-83 and apoA-I 1-83/G26R in the presence of oxidized phospholipids.

System	F_{max}, a.u.	t_m, h	$k \cdot 10^{-3}$, h^{-1}	Lag time, h	R^2
1-83	133	90	29	21	0.995
1-83 + PazePC (1:10)	-	-	-	-	-
1-83 + PoxnoPC (1:10)	54	176	15	43	0.994
1-83/G26R	71	19	188	8	0.997
1-83/G26R + PazePC (1:10)	-	-	-	-	-
1-83/G26R + PazePC (1:1)	105	38	131	23	0.997
1-83/G26R + PazePC (10:1)	55	30	115	13	0.994
1-83/G26R + PoxnoPC (1:10)	129	35	92	13	0.994
1-83/G26R + PoxnoPC (1:1)	290	28	119	11	0.992
1-83/G26R + PoxnoPC (10:1)	191	34	200	24	0.997
1-83/G26R + POPC	156	132	53	94	0.999
1-83/G26R + POPC/PazePC(20 mol%)	110	125	36	69	0.999
1-83/G26R + POPC/PoxnoPC(20 mol%)	158	125	42	77	0.999

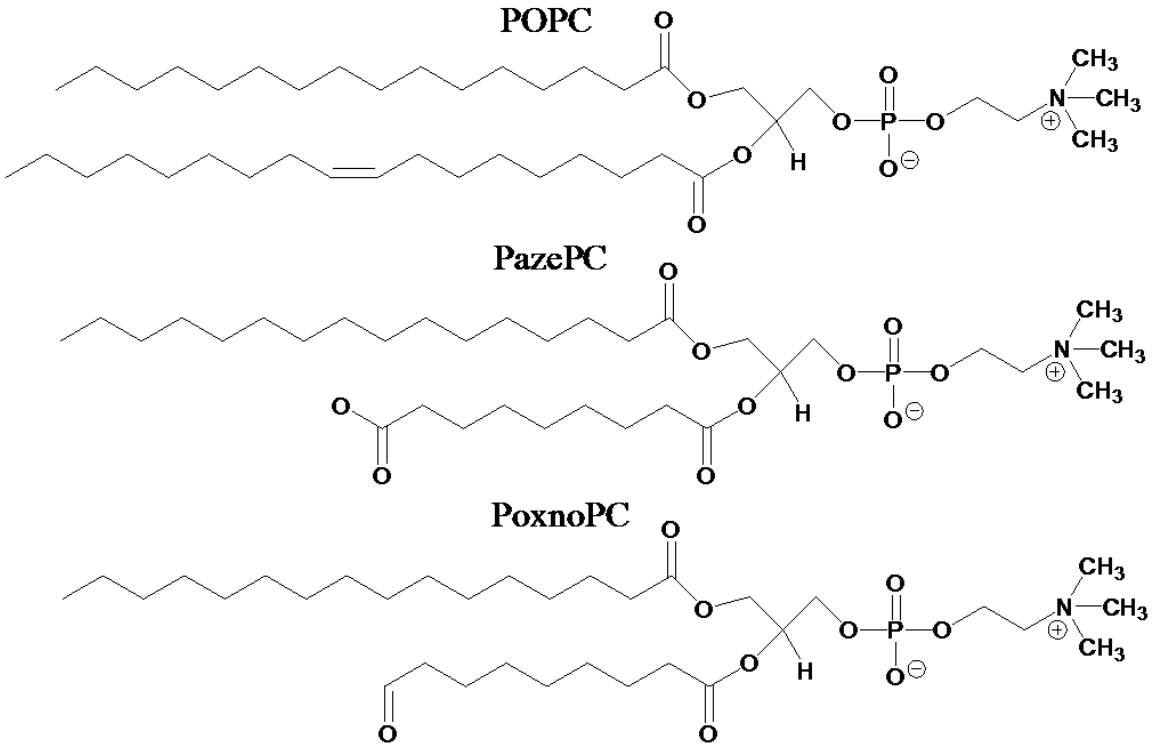

Fig. 1

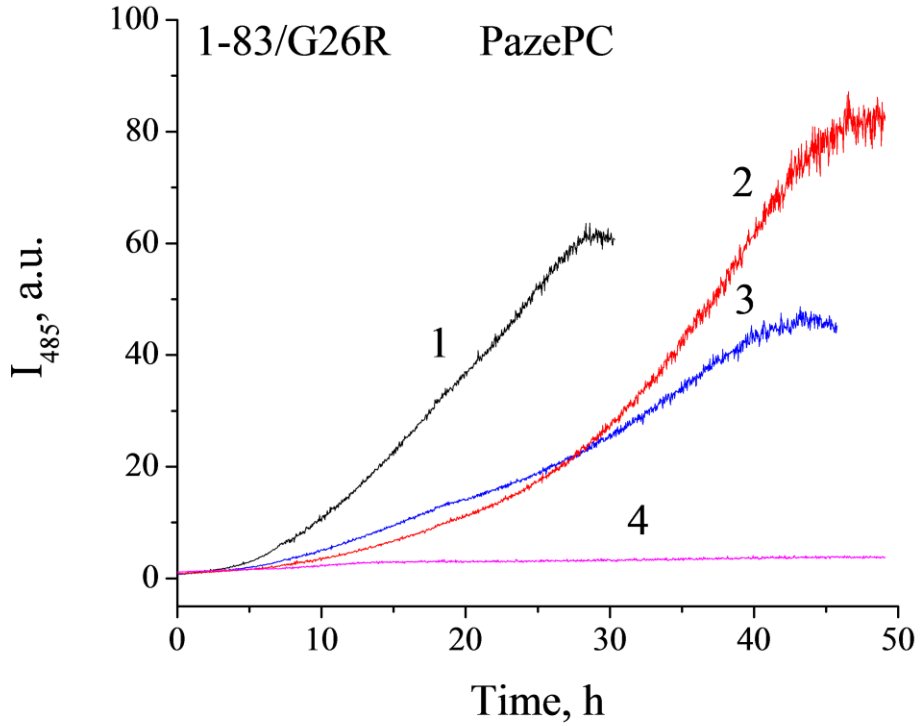
1-83/G26R
PazePC
I_{485}, a.u.
Time, h
1
2
3
4
0
20
40
60
80
100
0
10
20
30
40
50

Fig. 2A

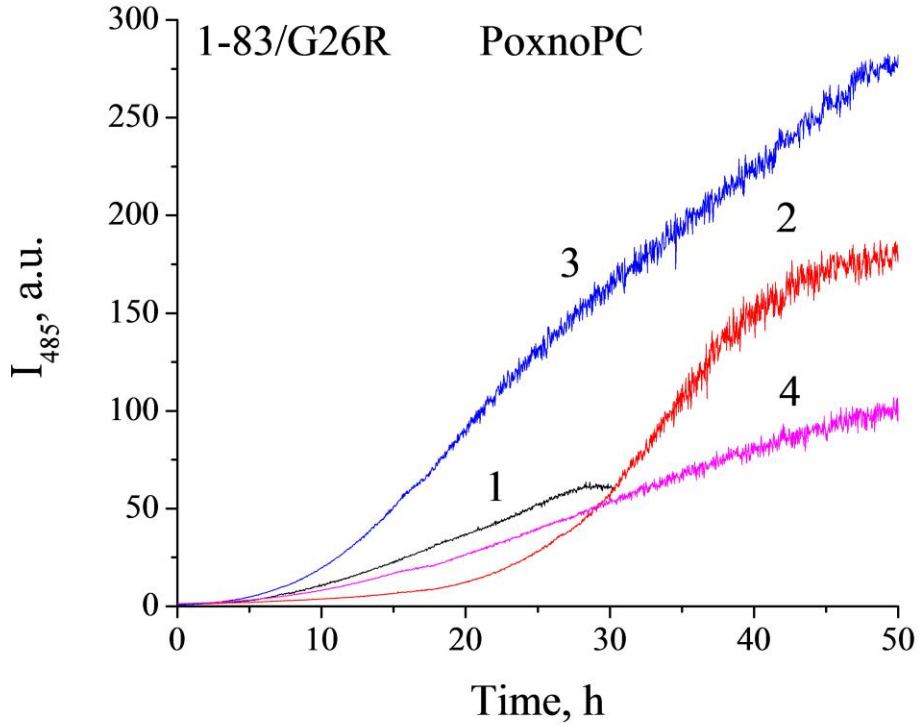
1-83/G26R
PoxnoPC
I_{485}, a.u.
Time, h
1
2
3
4
0
50
100
150
200
250
300
0
10
20
30
40
50

Fig. 2B

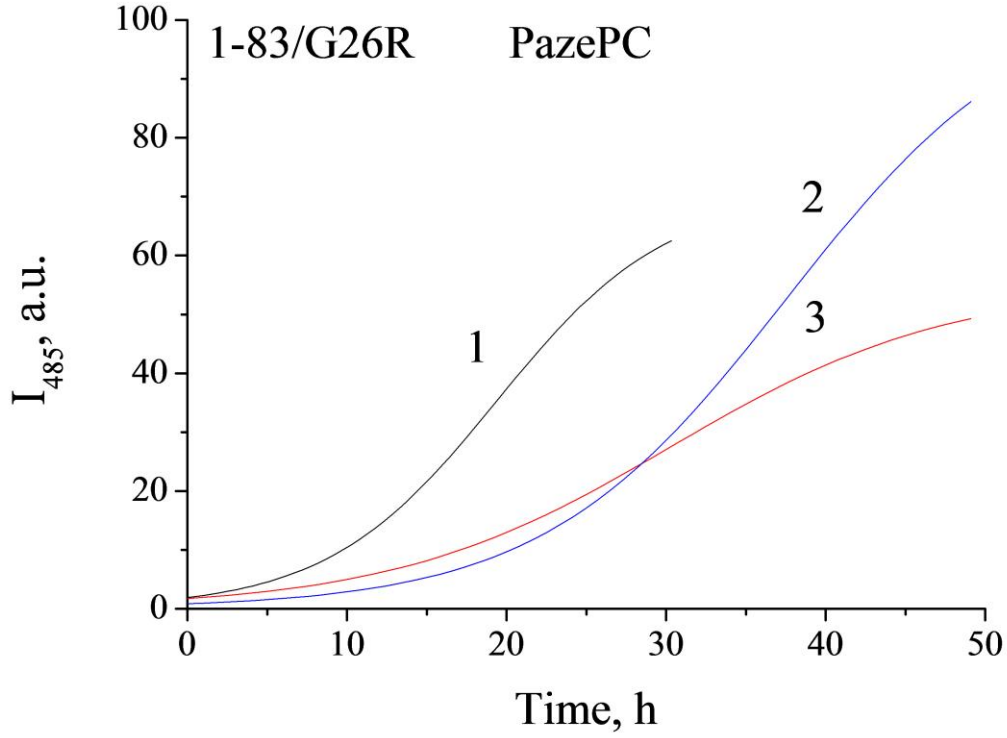
1-83/G26R PazePC
I_{485}, a.u.
Time, h
1
2
3
0
20
40
60
80
100
0
10
20
30
40
50

Fig. 2C

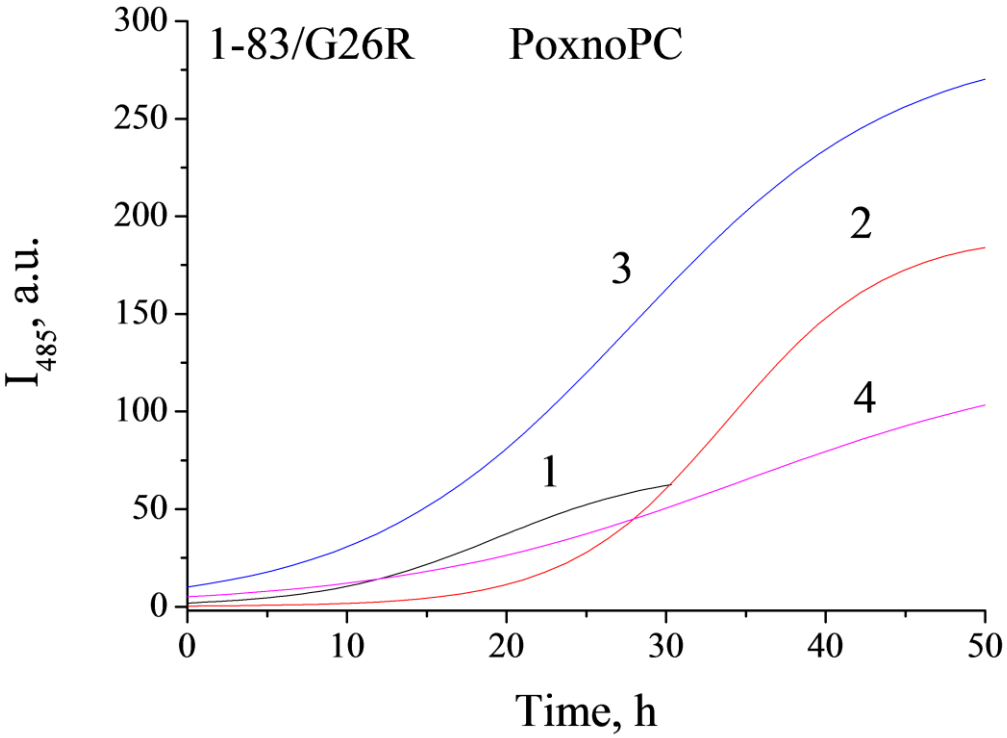
1-83/G26R PoxnoPC
I_{485}, a.u.
Time, h
1
2
3
4
0
50
100
150
200
250
300
0
10
20
30
40
50

Fig. 2D

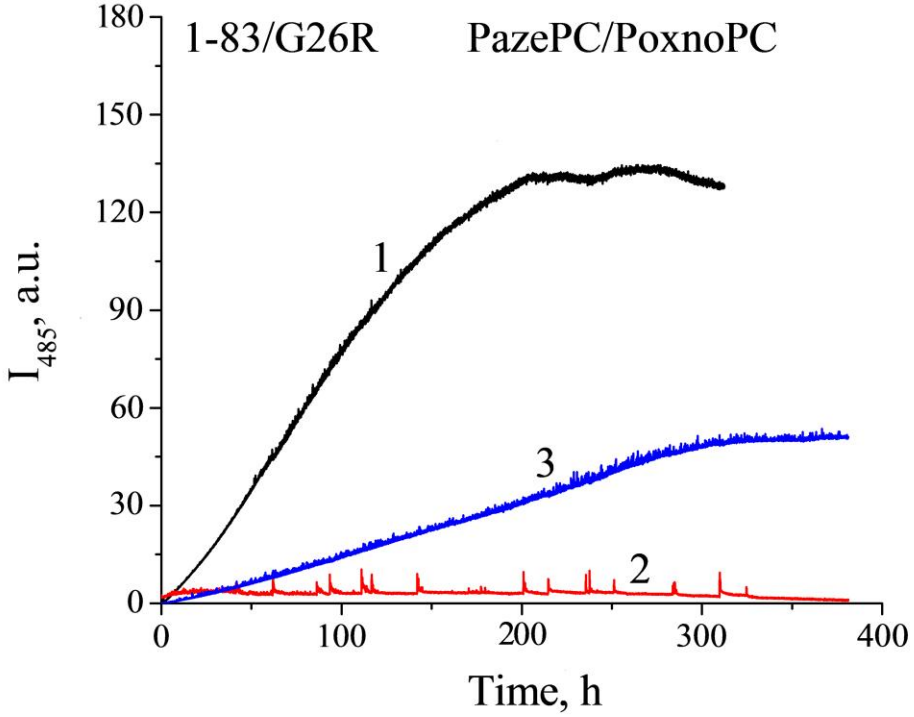
1-83/G26R
PazePC/PoxnoPC
I_{485}, a.u.
Time, h
1
2
3
0
30
60
90
120
150
180
0
100
200
300
400

Fig. 3A

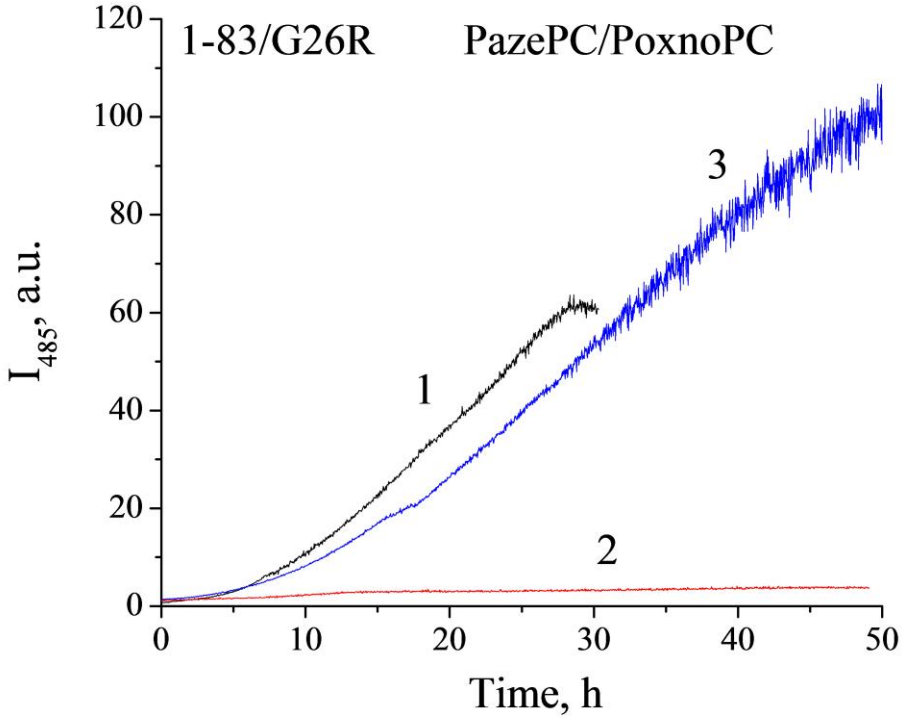
1-83/G26R
PazePC/PoxnoPC
I_{485}, a.u.
Time, h
1
2
3
0
20
40
60
80
100
120
0
10
20
30
40
50

Fig. 3B

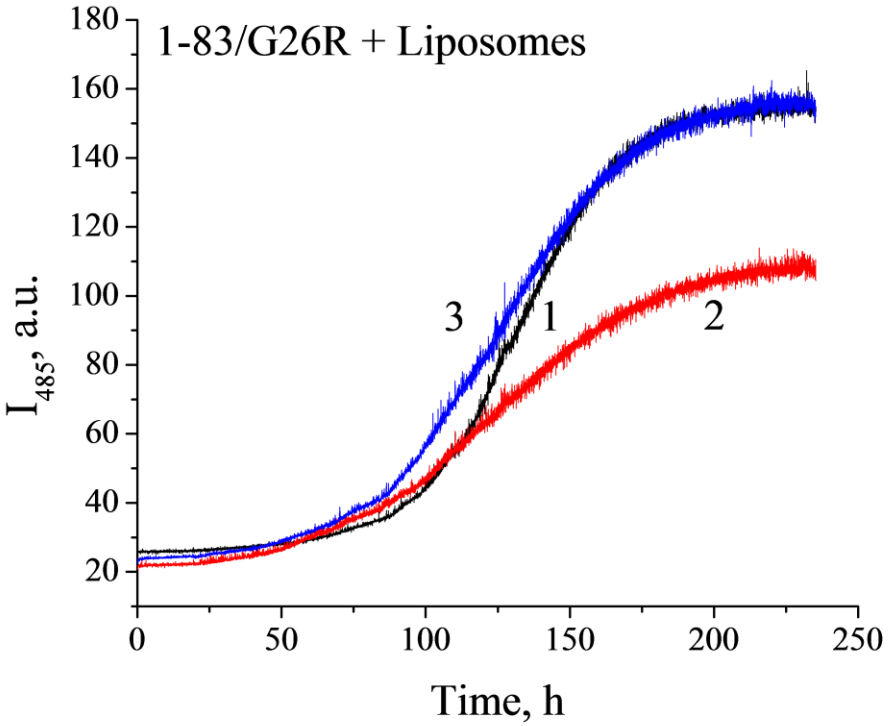
1-83/G26R + Liposomes
I_{485}, a.u.
Time, h
1
2
3

Fig. 4A

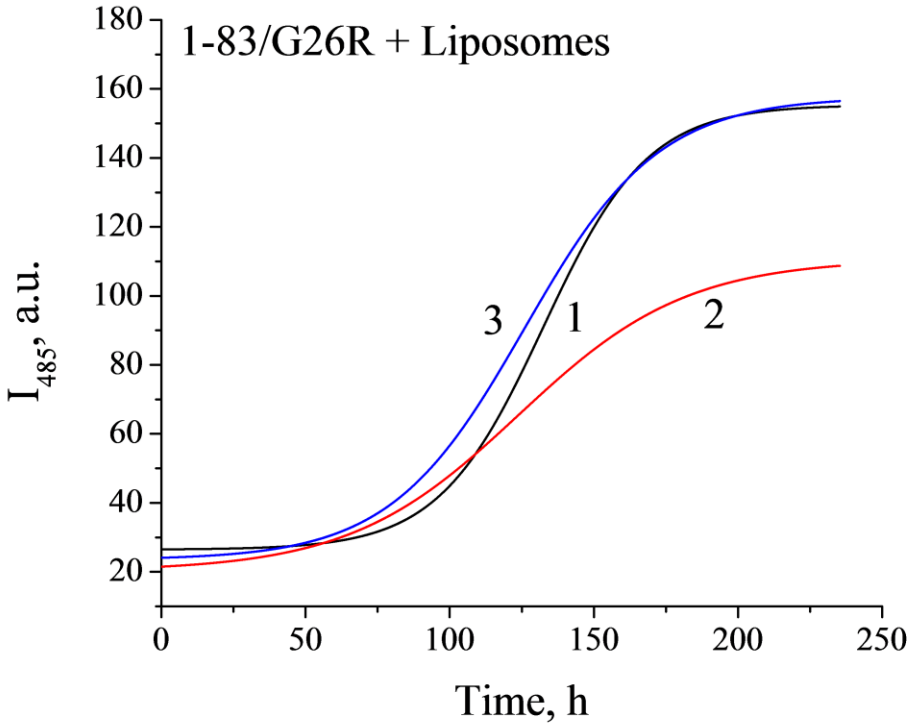
1-83/G26R + Liposomes
I_{485}, a.u.
Time, h
1
2
3

Fig. 4B

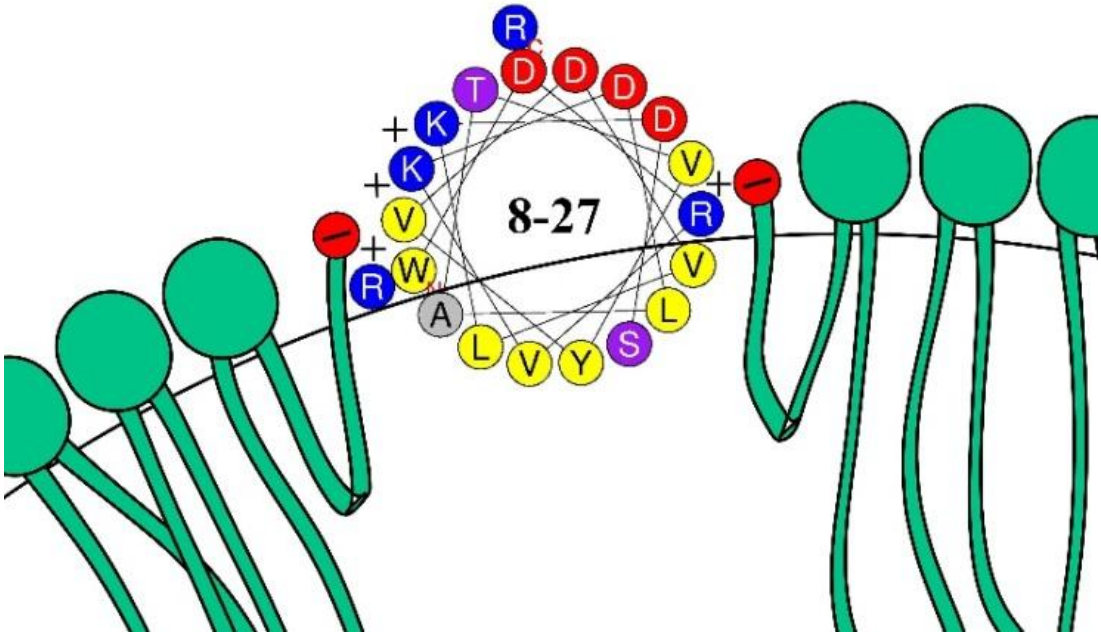

Fig. 5A

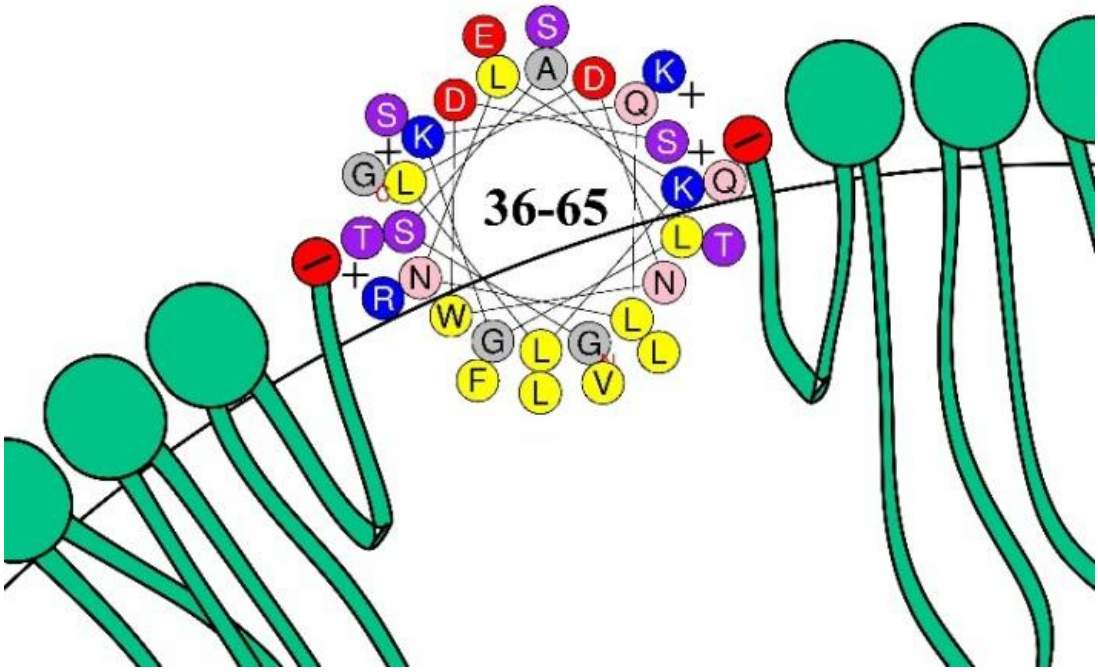

Fig. 5B